

# Microbialite-induced mats in siliciclastic Plio-Quaternary? sediments of NW Iberia

*Mantos inducidos por microbialitas en sedimentos siliciclásticos plio-cuaternarios? del NO de Iberia*

Javier Fernández-Lozano<sup>1</sup>, Pablo Caldevilla<sup>1</sup>, Fernando Gómez-Fernández<sup>1</sup> and Antonio Bernardo-Sánchez<sup>2</sup>

<sup>1</sup> Área de Prospección e Investigación Minera. E.S.T.I. Minas. Universidad de León. Campus VegaZana s/n, 24007, León. jferl@unileon.es; pcald@unileon.es; f.gomez@unileon.es

<sup>2</sup> Área de Explotación de Minas. E.S.T.I. Minas. Universidad de León. Campus VegaZana s/n, 24007, León. antonio.bernardo@unileon.es

## ABSTRACT

*Microbial mats are organo-sedimentary deposits formed by bacteria that trap or synthesize certain chemical elements. This type of activity gives rise to the formation of lamellar and/or columnar bioconstructions (stromatolites) and/or concentric structures (oncolites and thrombolites). The study of microbial mats used to be restricted mainly to marine and coastal environments related to the formation of ancient carbonate sediments (Palaeozoic/Proterozoic), and/or extreme conditions in hypersaline environments. However, in recent years, the presence of these forms has been identified in continental siliciclastic rocks and sediments with a temporal distribution that reaches into modern times. In this study, several levels of ferruginous crusts associated with microbial activity are found, interspersed in a Cenozoic deposit located in the province of Zamora. This deposit consists of concentric, laminated iron structures filled with silt, interspersed throughout a clayey-silt layer of variegated colors which shows signs of bioturbation and desiccation due to fluid escape. These findings allow the inference of the sedimentary and climatic conditions responsible for the growth and preservation of microbial mats in the siliciclastic sediments of the north-western edge of the Duero Basin.*

## RESUMEN

*Los mantos microbianos constituyen depósitos organosedimentarios formados por bacterias que atrapan o sintetizan determinados elementos químicos. Este tipo de actividad da lugar a la formación de estructuras laminares y/o columnares (estromatolitos) y/o concéntricas (oncolitos y trombolitos). Su estudio, por tanto, quedaba reducido principalmente a ambientes marinos y litorales relacionados con la formación de sedimentos carbonatados de edad muy antigua (Paleozoico/Proterozoico), y/o condiciones extremas en ambientes hipersalinos. Sin embargo, en los últimos años, se ha identificado la presencia de estas formas en rocas y sedimentos de afinidad continental y carácter siliciclástico, que se extienden temporalmente hasta la actualidad. En este estudio, se presenta el hallazgo de varios niveles de costras ferruginosas asociadas a la actividad microbiana, intercalados en un depósito cenozoico de la provincia de Zamora. Se trata de una serie de niveles caracterizados por la presencia de capas ferruginosas laminadas y concéntricas, constituidas por limos que aparecen en el techo y muro de un nivel arcilloso-limoso de colores abigarrados y signos de bioturbación y desecación por escape de fluidos. Este singular hallazgo permite establecer las condiciones sedimentarias y climáticas responsables del crecimiento y conservación de mantos microbianos en sedimentos siliciclásticos del borde noroccidental de la cuenca del Duero.*

**Key-words:** microbialite, siliciclastic stromatolites, NW Iberia, Cenozoic.

**Palabras clave:** microbialitas, estromatolitos siliciclásticos, noroeste ibérico, Cenozoico.

Geogaceta, 68 (2020), 51-54

Fecha de recepción: 30/01/2020

ISSN (versión impresa): 0213-683X

Fecha de revisión: 23/04/2020

ISSN (Internet): 2173-6545

Fecha de aceptación: 29/05/2020

## Introduction

The presence of iron deposits in the NW border of the Duero basin has been often associated with a process of hydro-morphism during successive wet-dry cycles in paleosoils, leading to the fixation of Fe and Mn oxyhydroxides (Alonso-Gavilán *et al.*, 1989; Molina and Martín-Serrano, 1991). However, a reinterpretation of this type of sedimentary facies has linked them to microbial-mats induced by the biological activity carried out by microbes (García-Hidalgo *et al.*, 2018).

The start of biological activity on land 3480 million of years ago (Djokic *et al.*, 2017), experienced a rapid development in continental environments, where the supply of terrigenous materials pre-

dominates, and carbonate deposition is insignificant or even non-existent. Martín *et al.* (1993) defined stromatolites and siliciclastic thrombolites as those with more than 10% of siliciclastic particles in their composition.

In Spain, stromatolites have been studied in several continental environments: ferromagnesian stromatolites in caves (Rossi *et al.*, 2016); silicic stromatolites in fluvial currents (Arenas *et al.*, 2019), as well as the dolomite and silica-rich stromatolites in the Duero Basin (Sanz-Montero *et al.*, 2008). This work addresses the study of the formation of ferruginous microbial structures in a continental setting during the upper Miocene (Plio-Quaternary? according to the similarities with the sediments found in the nearby Eria valley,

Fernández-Lozano *et al.*, 2016). The studied sequence represents a sedimentary environment dominated by siliciclastic deposits with interbedded laminar and dome-shaped ferruginous layers, whose genesis is linked to biomineralization processes responsible for the fixation of iron oxides.

## Geological framework

The study area is located in the vicinity of Villalverde, in the region of La Carballeda (Zamora). It lies in the Ollo de Sapo Domain, in the Central Iberian Zone of the Iberian Massif (Julivert *et al.*, 1974). The Alpine tectonic uplift of the Appalachian reliefs, composed of low-Ordo-vician slates and quartzites (Armorican

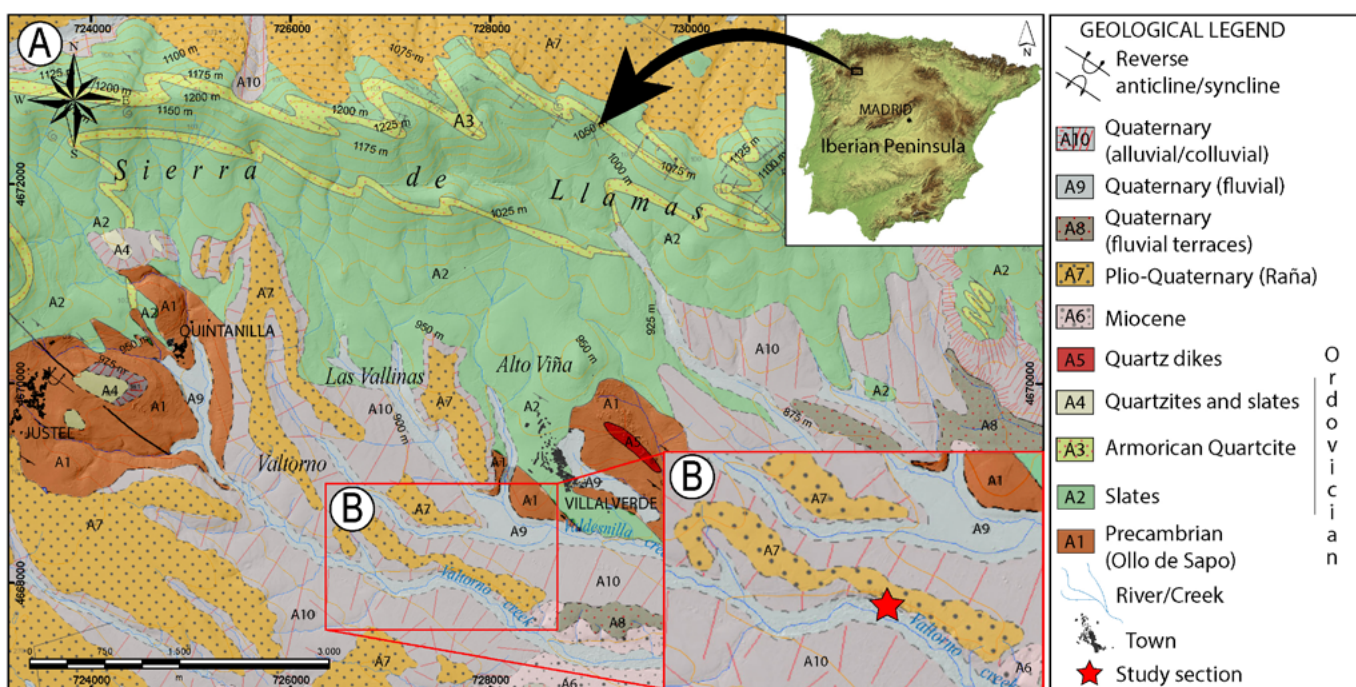


**Fig. 1.- A) General geological map. Modified after González et al. (1981). B) Detailed geological sketch map of the study area. See color figure in the web.**

Fig. 1.- A) Mapa geológico general. Modificado de González et al. (1981). B) Esquema geológico detallado de la zona de estudio. Ver figura en color en la web.

facies), gave rise to several peneplain surfaces, also known as rañas (Fig. 1). Rañas are slightly inclined surfaces ( $< 5^\circ$ ) and represent the remains of alluvial fans, from which the fluvial incision of the Valtorno creek started (Fig. 1).

Rañas comprise a group of conglomerates with subangular-rounded pebble-cobble sized clasts in a reddish-orange matrix and black pebbles, which link the plateau to the Paleozoic reliefs in the north throughout extensive meseta areas (Martín-Serrano, 1991). The underlying sequence comprises a group of upper Miocene sediments composed of an alternation of silty-clays and conglomerates with interbedded sandy channels that have been dated by correlation with nearby basins based on the fossil content (Alberdi and Aguirre, 1970). These materials rest unconformably over the Cambro-Ordovician metamorphic rocks (slates and glandular gneisses).

## Methodology

Firstly, a stratigraphic column was generated (Fig. 2), and paleocurrent directions and imbricated conglomerate clasts were measured. Then, a petrographic characterization was done on three different polished thin sections from laminated and dome-shaped structures. In addition, samples were analyzed using a JEOL

JSM-6480 scanning electron microscope (SEM), equipped with an Oxford D6679 Energy-dispersive X-ray (EDS) detector, which provided qualitative and quantitative data on sample composition. For this purpose, polished thin sections were previously covered with pulverized carbon.

## Results and discussion

The iron-rich sequences are intercalated between the upper levels of the Miocene conglomerates and the bottom of the raña, within the silty-clays (Fig. 2). The lower reaches form laminar structures 10–15 cm thick that wedge towards the sides, while the upper part ( $\approx 1$  m), in contact with the silts and clays, comprises a series of dome-like structures that end up into laminar structures (Figs. 3A and B).

Domes are 10–30 cm wide and comprise finely laminated, concentric structures. The uppermost level is composed of limonite-rich layers that are also finely laminated.

The thin section analysis shows the presence of angular quartz grains (monomineral), quartzite-slate lithic clasts and accessory minerals intercalated within the laminar structures (Figs. 3D and E). These laminae comprise a whole range of light-grey tones in the BSE-SEM image and are mostly iron oxides (Table I; see Fig. 4 for location of EDS analysis).

The presence of phosphorous here is suggestive of the organic origin of these laminar structures (Rao et al., 2000). An iron-rich matrix coats the angular quartz grains, which show little displacement, indicating proximal source area for the origin of the quartz grains (Fig. 4). In some cases, the slate fragments are partially or totally altered, replacing chlorite by iron-oxides, eventually responsible for the reddish colour of the matrix of the sediments containing the laminar structures. This process of rubefaction has been previously identified in the nearby area of the Eria river basin (León) by Fernández-Lozano et al. (2016).

The iron-rich laminar bodies are interpreted to be microbial-mats that trap the fine grain sediments (Fig. 3F). Compare the spectrums from two different laminar bodies in figure 4 and table I. Similar examples have been identified in the Iberian Range by García-Hidalgo et al. (2018). Their growth is controlled by the water table, giving rise to laminae or domal structures (over 40 cm high), during the periods of waterlogging or drought, respectively (Fig. 3A). The observed presence of upright structures affecting the lamination has been related to fluid escape structures (Fig. 3C), suggesting the presence of early diagenetic processes; whereas marks of root footprints associated with the silty clay indicate periods

of subaereal exposure (Fig. 3A), characteristic of paedogenetic conditions in an ancient river floodplain. Also examples of these structures were described in fluvial deposits of 3200 Ma in South Africa (Hommann *et al.*, 2018). Other examples have been documented in association with siliciclastic sediments (Surdam and Wray, 1976; Fedorchuk *et al.*, 2016) and iron-rich biogenic precipitation (Chang *et al.*, 1989).

It is important to note that these structures are scarce in the fossil record and their remarkable preservation in these deposits is due to their iron-rich composition. Present-day microbialite mats have been described in environments with high iron content, particularly the stromatolite structures associated with the activity of the *Thiobacillus ferroxidans* bacteria in acid mine drainage (Leblanc *et al.*, 1996; Brake *et al.*, 2014). Therefore, the origin of the structures we observe here is most likely the synthesis and concentration of iron precipitates that occurred during the metabolic activity of bacteria.

## Conclusions

The sedimentary structures found in the Valtorno valley (Villalverde, Zamora) represent an outstanding example of microbial mats in siliciclastic sediments. They are associated with bacteria, which are responsible for the iron-oxide biominerization and binding of fine silt particles and show evidence for repeated episodes of flooding and subaereal exposition. These conditions are characteristic of the arid climates of the past. Their identification allows for the reconstruction of the sedimentary and climatic conditions of the western end of the Duero Basin during the Cenozoic era.

## Acknowledgements

This work was partially funded by the Projects 0284\_Esmimet\_3\_E (Interreg V-A Programa de Cooperación España-Portugal, 2014-2020) and LE167G18 (Junta de Castilla y León, Spain). Authors are indebted to Francisco Bajo Álvarez, the Editor and two anonymous reviewers for their comments and suggestions.

## References

Alberdi, M.T. and Aguirre, E. (1970). *Estudios Geológicos* 36, 401-415.

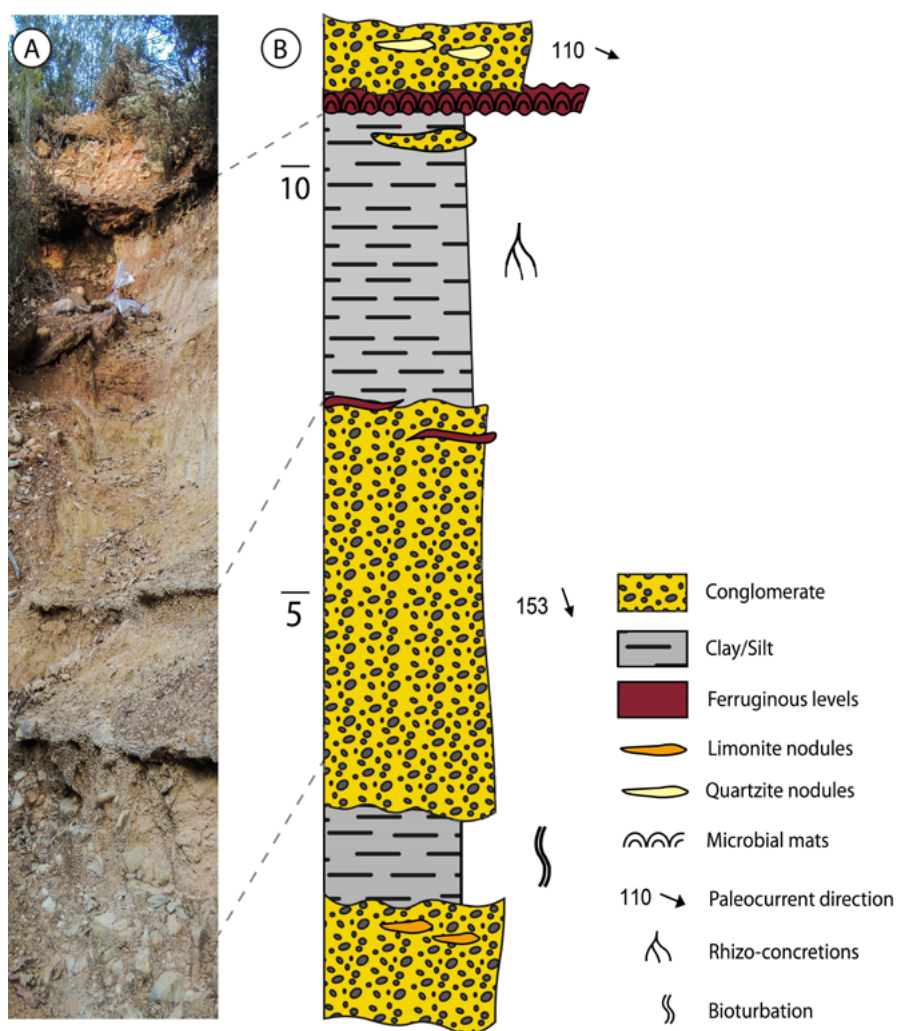


**Fig. 2.- A)** Image of the upper part of the studied section (not to scale). **B)** Complete stratigraphic column of the studied section. Vertical distance in meters. See color figure in the web.

**Fig. 2.- A)** Fotografía del tramo superior de la sección estudiada (no está a escala). **B)** Columna estratigráfica completa de la sección estudiada. Distancia vertical en metros. Ver figura en color en la web.

Sp 1	Sp 2	% W	Error ( $\sigma$ )
Fe	Fe	28,9	50,8
O	O	43	38,3
Al	Al	10,3	4,9
Si	Si	14,7	4,8
K	K	2,8	0,6
P	P	0,2	0,8

**Table I.- Composition (% weight) from spectrum 1 and 2 taken from the same sample imaged in figure 4,  $\sigma$  is standard deviation of the measurement.**

**Tabla I.- Composición (% peso) obtenido de los espectros 1 y 2 en la figura 4,  $\sigma$  es la desviación estándar de precisión en la medida.**

- Alonso Gavilán, G., Blanco Sánchez, J.A., Sánchez Macías, S., Fernández Macarro, B. and Santisteban Navarro, J.I. (1989). *Studia Geológica Salmanticensia* 5, 187-207.  
Arenas, C., Osácar, M.C., Auqué, L. and Sancho, C. (2019). *Journal of Palaeogeography* 8, 1-20.

Brake, S.S., Arango, I., Hasiotis, S.T. and Burch, K.R. (2014). *Environmental Earth Sciences* 72, 2779-2796.

Chang, S.B.R., Stoltz, J.F., Kirschvink, J.L. and Awramik, S.M. (1989). *Precambrian Research* 43, 305-315.

Djokic, T., Van Kranendonk, M.J., Campbell, K.A., Walter, M.R. and Ward, C.R. (2017). *Nature Communications* 8, 15263.

Fedorchuk, N.D., Dornbos, S.Q., Corsetti, F.A., Isbell, J.L., Petryshyn, V.A., Bowles, J.A. and Wilmet, D.T. (2016). *Precambrian Research* 275, 105-118.

Fernández-Lozano, J., Blanco-Sánchez, J.A., García-Talegón, J. and Franco, P. (2016). *Geo-temas* 16, 371, 374.

García-Hidalgo, J.F., Elorza, J., Gil-Gil, J., Herrero, J.M. and Segura, M. (2018). *Sedimentary geology* 364, 24-41.

González, J.C., Monteserín, V. and Arce, J.M. (1981). *Mapa Geológico de España 1:50.000, hoja nº 268. (Molezuelas de la Carballeda) y memoria*. IGME, Madrid, 29 p.

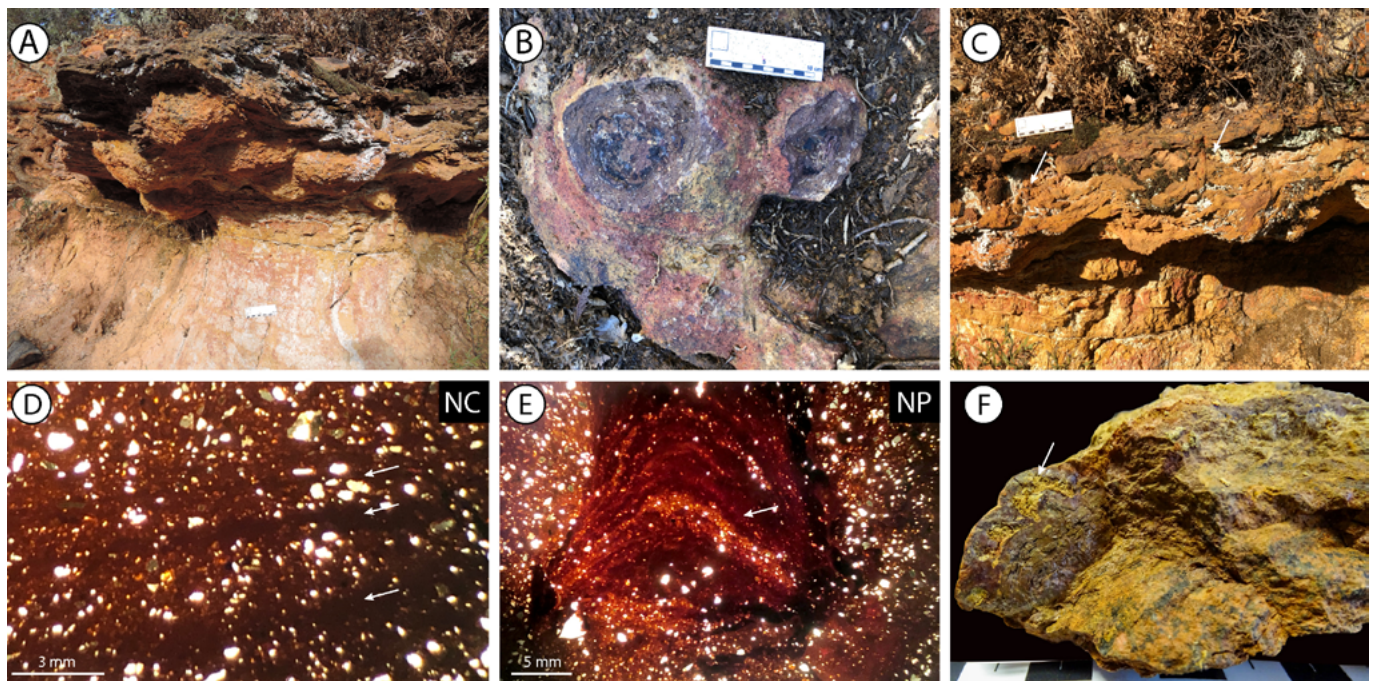


**Fig. 3.- A)** Contact between the clayey-silt level containing fossil plant roots and stromatolitic dome structures formed above laminar beds. **B)** Section of a group of algae domes showing concentric internal layering. **C)** Sedimentary escape structures in laminar levels (white arrows). **D)** Microphotography with crossed nicols showing where successive laminations by quartz grains and quartzite lithic grains have been bound due to bacterial activity (white arrows). **E)** Microphotography with plane polarised light showing columnar laminations with alternating iron-rich layers (white arrow) and layers composed of quartz grains covered with iron oxides. **F)** Photograph of a stromatolitic dome fragment composed of an iron-rich oxide coat and a silty infill (white arrow). See color figure in the web.

**Fig. 3.- A)** Contacto entre nivel limo-arcilloso con restos de raíces y estructuras de domos estromatolíticos que pasan a techo a niveles laminares. **B)** Sección de un grupo de domos algales donde se observan las sucesivas láminas internas que los conforman. **C)** Estructuras de escape en niveles laminares (flechas blancas). **D)** Microfotografía con nícolas cruzados donde se observan laminaciones sucesivas (flechas blancas), entre las que quedan atrapados granos de cuarzo, fragmentos líticos de cuarcita. **E)** Microfotografía con nícolas paralelos de algunas laminaciones observadas alternando capas ricas en óxido de hierro (flecha blanca) y capas compuestas por granos de cuarzo empastados en óxidos. **F)** Fotografía de un fragmento de domo estromatolítico donde se observan las envueltas algales ricas en óxido de hierro y el relleno limoso (flecha blanca). Ver figura en color en la web.

Homann, M., Sansjofre, P., Van Zuilen, M., Heubeck, C., Gong, J., Killingsworth, B., Foster, I., Airo, A., Van Kranendonk, M.J., Ader, M. and Lalonde, S.V. (2018). *Nature Geoscience* 11, 665-672.

Julivert, M., Fontboté, J., Ribeiro, A. and Nabais Conde, L.E. (1974). *Mapa Tectónico de la Península Ibérica y Baleares E: 1: 1.000. 000 y memoria explicativa*. Publ. IGME, Madrid, 113 p.

Leblanc, M., Achard, B., Othman, D.B., Luck, J.M., Bertrand-Sarfati, J. and Personné, J.C. (1996). *Applied Geochemistry* 11, 541-554.

Martín, J.M., Braga, J.C. and Riding, R. (1993). *Journal of Sedimentary Petrology* 63, 131-139.

Martin-Serrano, A. (1991). *Revista de la Sociedad Geológica de España* 4, 337-351.

Molina, E. and Martín-Serrano, A. (1991). In: *Alteraciones y paleoalteraciones en la morfología del oeste peninsular* (E. Molina, Ed.). IGME, Salamanca, 251-262.

Rao, V.P., Rao, K.M. and Raju, D.S.N. (2000). *Journal of Sedimentary Research* 70, 1197-1209.

Rossi, C., Villalaín JJ., Lozano R.P. and Hellstrom J. (2016). *Geomorphology* 261, 57-75.

Sanz-Montero, M.E., Rodríguez-Aranda, J.P. and García del Cura, M.A. (2008).

*Sedimentology* 55, 729-750. Surdam, R.C. and Wray, J.L. (1976). *Developments in Sedimentology* 20, 535-541.

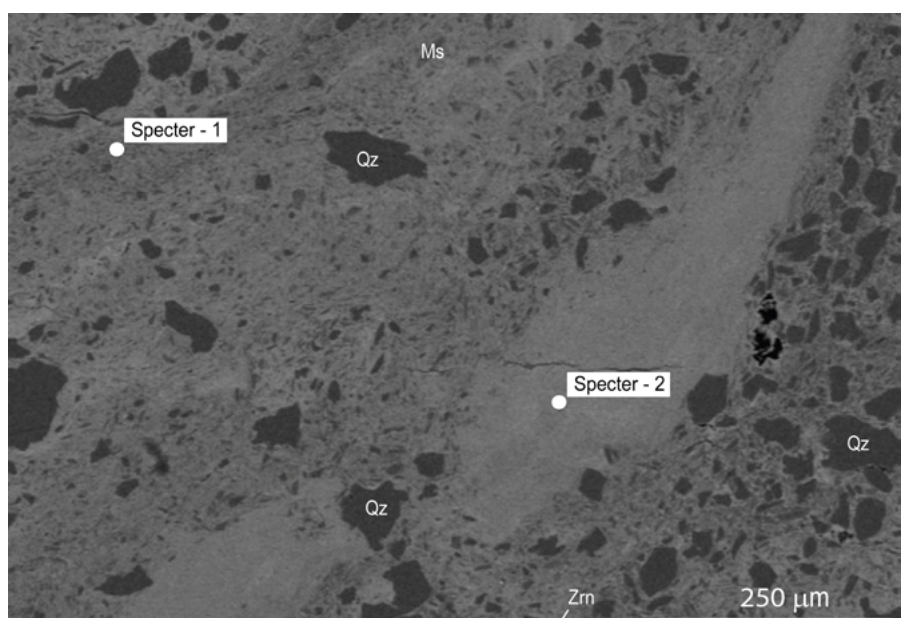


**Fig. 4.-** BSE-SEM image showing iron-oxide lamination involving quartz (Qz), muscovite (Ms) and zircon (Zrn). The location of the EDS analysis points is shown (Specter 1 and 2). See figure color in the web.

**Fig. 4.-** Imagen de electrones retrodispersados, donde se observa la laminación formada por óxidos de hierro que incorporan granos de cuarzo (Qz), mica moscovita (Ms) y zircón (Zrn). Se muestran los puntos de análisis EDS (Espectro 1 y 2). Ver figura en color en la web.